Hindawi
Mathematical Problems in Engineering
Volume 2020, Article ID 8642430, 12 pages
https://doi.org/10.1155/2020/8642430

Research Article

Predicting Ink Transfer Rate of 3D Additive Printing Using EGBO Optimized Least Squares Support Vector Machine Model

Shengpu Li[1,2] and Yize Sun[3]

[1]*College of Information Science and Technology, Donghua University, Shanghai 201620, China*
[2]*College of Information Engineering, Pingdingshan University, Pingdingshan 467002, China*
[3]*College of Mechanical Engineering, Donghua University, Shanghai 201620, China*

Correspondence should be addressed to Yize Sun; sunyz_dhu@163.com

Received 18 June 2020; Revised 4 September 2020; Accepted 15 September 2020; Published 25 September 2020

Academic Editor: Francesco Clementi

Ink transfer rate (ITR) is a reference index to measure the quality of 3D additive printing. In this study, an ink transfer rate prediction model is proposed by applying the least squares support vector machine (LSSVM). In addition, enhanced garden balsam optimization (EGBO) is used for selection and optimization of hyperparameters that are embedded in the LSSVM model. 102 sets of experimental sample data have been collected from the production line to train and test the hybrid prediction model. Experimental results show that the coefficient of determination (R^2) for the introduced model is equal to 0.8476, the root-mean-square error (RMSE) is $6.6 \times 10\ (-3)$, and the mean absolute percentage error (MAPE) is $1.6502 \times 10\ (-3)$ for the ink transfer rate of 3D additive printing.

1. Introduction

The quality of the vamp printed by the traditional running table depends entirely on the using experiences of the printer, so the printing quality stability is poor when different people use the printer. A good way to get better quality and stability of printing is intelligent parameter adjusting of the 3D additive printing machine. In the practical production, squeegee angle, printing pressure, squeegee speed, ink viscosity, and screen mesh thickness affect the adhesion of ink from screen to sneaker surface and then directly affect the printing quality of vamp [1]. Adjusting all of these influencing factors that are parameters of the printing machine should be important and can be considered in the production process of 3D additive printing. Therefore, the study on the optimization of parameter adjusting of 3D printing machine is of great significance to realize the high-precision printing of 3D printing machine and improve quality and stability of printing.

In the case of unchanged printing screen, there are four adjustable parameters of the printing machine, such as the squeegee angle, printing pressure, squeegee speed, and ink viscosity [2]. In the practical production, the additive printing process (that is, the ink adhesion through the screen surface attached to the process) directly determines the printing quality of the product. Generally the product quality is higher when ink adhesion is more; the product quality is lower when ink adhesion is less. Therefore, ink transfer rate (ITR) can be used as an evaluation standard to measure the quality of printing. Therefore, it is necessary to establish a prediction model based on experimental data to obtain the optimal process parameters [3].

Based on the above analysis, the process parameter optimization problem of 3D additive printing can be described as the mathematical model as following. The squeegee angle, printing pressure, squeegee speed, and ink viscosity are four input parameters in the model, ITR is the output of the printing effect index, and the goal of the model is finding out the relationship between the input parameters and output index [4]. According to this model, the optimal parameter combination can be found from input parameter combination evaluating. In 3D additive printing, the model

which builds the relationship between input parameters and output index has become the important and difficult optimization problems. As shown in previous studies [5], the difficulty is that the mapping between the input parameters and the printing effect index is highly nonlinear.

Because of the importance of the research topic, the production staff tried to do a lot of work on the experiment of improving the printing quality by the combination of process parameters. Machine learning as an advanced modeling tool has been used effectively in engineering applications [6–12]. Wang et al. [5] divided the four process parameters into five levels to design the orthogonal experiment and divided the printing quality evaluation into five levels to obtain a group of relative optimal process parameter combination through comparative analysis. On the basis of the former research, Wang et al. [13] used the artificial neural network (ANN) model to study the experimental database of 102 production test results and built a network model for quality prediction.

According to the literature review, the application of advanced machine learning-based model to estimate printing quality remains a rarity. Although other methods such as ANN and gene expression programming (GEP) can also be used for printing quality modeling, these methods also have certain difficulties [14]. The neural network model is established by using the gradient descent method and the back propagation algorithm, which means that their training stage is easy to fall into the local optimum. In addition, although GEP can automatically construct prediction equations, the prediction accuracy of this machine learning method may not be as good as that of ANN. Therefore, the paper is to study the ability of other advanced machine learning methods, which should be studied to improve prediction accuracy.

In this study, the least squares support vector machine (LSSVM) is used to construct a functional mapping to solve the above difficult printing quality prediction problem [15]. As a powerful nonlinear and multivariate modeling tool, LSSVM is used to solve engineering mathematical problems [16]. However, determining an appropriate set of LSSVM model hyperparameters can be a challenging task because of the myriad of solution candidates [17]. Since the setting of LSSVM model hyperparameters can be modeled as optimization tasks, the garden balsam optimization (GBO) algorithm is used. On this basis, the performance of the LSSVM and GBO hybrid model in printing quality modeling is studied. The reason why GBO is chosen in this study is that GBO is a relatively new algorithm with good optimization performance [18]. 102 data samples have been collected from the experiment, including four input factors, such as printing pressure, squeegee angle, squeegee speed, and ink viscosity, to train and test the LSSVM model. In addition, since most of the previous work on printing quality estimation only relied on individual machine learning algorithms, one of the main contributions of this study is proposing a hybrid model to improve the accuracy by mixing machine learning and swarm intelligence optimization methods.

The chapters of this paper are organized as follows: the next part reviews the calculation methods used by LSSVM and GBO to build the hybrid prediction model. The third part describes the proposed model. The fourth part reports the experimental results. The concluding remarks are provided in the last section.

2. The Employed Computational Intelligence Methods

2.1. Least Squares Support Vector Machine (LSSVM). This section describes the LSSVM method used to construct a mapping function between the ITR and technological parameters. The LSSVM is a powerful nonlinear function approximation method that can effectively process multivariable and small-scale datasets [19]. This machine learning approach first performs data transformation, mapping data from the original input space to the higher-dimensional feature space [20]. Therefore, a linear model can be constructed in the eigenspace to infer the mapping relationship between response variables and a set of independent variables.

In addition, the radial basis function (RBF) kernel is commonly used in LSSVM [10]. It is worth noting that in addition to the RBF kernel, other functions such as linear or polynomial kernels can also be applied. However, in previous applications, the RBF kernel has been shown to have satisfactory learning performance [10]. Therefore, this paper chooses this kernel function to study.

LSSVM is a mature technology, and I will not go into details here. The model for the LSSVM method requires setting two hyperparameters, such as the regularization coefficient (γ) and the kernel function parameter (σ). The randomness of these two parameters is relatively large, and there is no certain law to follow. Intelligent optimization algorithms can be used to solve this problem [21, 22].

2.2. Enhanced Garden Balsam Optimization (EGBO). Garden balsam optimization (GBO) is a recent swarm-based evolutionary algorithm that is inspired by the seed transmission mode of garden balsam. Garden balsam randomly ejects the seeds within a certain range by virtue of mechanical force originating from cracking of mature seed pods, which is different from natural expansion of most species of plants. The seeds scattered to suitable growth area will have greater reproductive capacity in the next generation, followed by iteration until the most suitable point for growth in a particular space is eventually found. Like other evolutionary algorithms, GBO is a numerical random search algorithm that simulates natural behavior. However, it also shows some deficiencies in the experiment. In the iteration process of the basic GBO algorithm, there is no cooperative mechanism between individuals; furthermore, there is lack of utilization of optimal individual information.

In the algorithm improvement, the balance between the early global exploration capability and the later local development capability should be considered. Enhanced

garden balsam optimization (EGBO) uses flower pollination strategy for the population [23, 24]. This flower pollination strategy depends on the strength of the pollination. There are two key steps in this strategy: global pollination and local pollination.

In the global pollination step, flower pollens are carried by pollinators such as insects, and pollens can travel over a long distance. This ensures the pollination and reproduction of the most fit, and thus, we represent the most fit as G_{best}^t. The first rule can be formulated as follows:

$$X_i^* = X_i^t + L\left(G_{\text{best}}^t - X_i^t\right), \tag{1}$$

where X_i^t is the solution vector i at iteration t and G_{best}^t is the current best solution. The parameter L is the strength of the pollination which is the step size randomly drawn from Lèvy distribution [24]. This paper draws $L > 0$ from a Lèvy distribution as follows:

$$L \sim \frac{\lambda\Gamma(\lambda)\sin(\pi\lambda/2)}{\pi} \times \frac{1}{s^{1+\lambda}}, \quad s \gg s_0 > 0, \tag{2}$$

where $\Gamma(\lambda)$ is the standard gamma function, and this distribution is valid for large steps$s > 0$. In all our simulations below, we have used $\lambda = 1.5$.

The local pollination and flower constancy can be represented as follows:

$$X_i^* = X_i^t + \varepsilon\left(X_j^t - X_k^t\right), \tag{3}$$

where X_j^t and X_k^t are pollens from the different flowers of the same plant species. This essentially simulates the stability of the flower in a finite neighborhood. Mathematically, if X_j^t and X_k^t come from the same species or selected from the same population, this becomes a local random walk if we draw ε from a uniform distribution in [0, 1]. To start with, we can use $p = 0.5$ as an initial value and then do a parametric study to find the most appropriate parameter range. From our simulations, we found that $p = 0.8$ works better for most applications.

The above two key steps plus the switch condition can be summarized in the pseudocode shown in Algorithm 1.

Based on the strategy, the EGBO algorithm flowchart is given in Figure 1. The detailed steps of the algorithm are as follows.

3. Framework of EGBO-LSSVM Model

This section describes the framework of the hybrid model used to predict the final ink transfer rate. The hybrid model combines EGBO and LSSVM. It is worth noting that LSSVM is used to build a functional map that calculates the final ink transfer rate value based on four input variables. Since the regularization coefficient and kernel function parameters need to be determined in the training phase of the LSSVM model, the EGBO clustering intelligent algorithm is adopted to set these two hyperparameters automatically.

Therefore, the hyperparameters of the LSSVM model are randomly generated within the above boundary, and their expressions are as follows:

$$P_i = L_i + \text{Rn} \times \left(U_i - L_i\right), \quad i = 1, 2, \tag{4}$$

where P_i is the i-th hyperparameter of the LSSVM model. Rn represents uniformly random numbers generated between 0 and 1. $L_i = 0.01$ and $U_i = 1000$ are the lower and upper bounds of the hyperparameter, respectively.

Figure 2 shows the overall concept of the hybrid EGBO-LSSVM model.

In order to determine the most appropriate LSSVM's hyperparameter set, k-fold cross validation is used in this study. To allow for the calculation of costs, let $k = 5$. Based on the cross-validation framework, the 102 sample data sets are divided into 5 data folds. The LSSVM predictive model is evaluated 5 times with each set of hyperparameters obtained by the EGBO algorithm. In each evaluation time, four data folds are used for model training, and the remaining one data fold is used for model prediction. The fitness function values are as follows:

$$\text{Fit} = \frac{\sum_{k=1}^{K} \text{Rm}_k}{K}, \tag{5}$$

where Rm_k denotes root-mean-square error (RMSE) of LSSVM.

RMSE is calculated as follows:

$$\text{Rm} = \sqrt{\sum_{i=1}^{N_K} \frac{\left(Y_{\text{A}} - Y_{\text{P}}\right)^2}{N_K}}, \tag{6}$$

where Y_{A} denotes actual value, Y_{P} denotes predicted value, and N_K denotes the number of samples.

After calculating the cost function for each member of the population, the EGBO algorithm performs mechanical and secondary propagators to explore the search space and find a better solution, and then updates the positions of all population members based on the elitist-random selection operator. The EGBO optimization continues until the number of iterations reaches the value of $\text{iter}_{\max}$. The optimized LSSVM model can be used to predict the ink transfer rate of new data samples when the appropriate set of hyperparameters is determined.

4. Experimental Results and Comparison

This section will present and analyze the experimental results of the hybrid EGBO-LSSVM model in the ink transfer rate prediction experiment. Four variables, including printing pressure ($X1$), squeegee angle ($X2$), squeegee speed ($X3$), and ink viscosity ($X4$), have been selected as input factors, and ink transfer rate (Y) has been selected to represent the printing quality of 3D additive printing machine. This data set has been summarized and recorded by Wang et al. [13]. Based on the literature review and available data, the assumptions of this study are as follows: (1) the ink transfer rate can be adequately modeled using the above four variables. (2) The current number of data samples is sufficient to meet the model construction and verification process.

The three variables of printing pressure ($X1$), squeegee angle ($X2$), and squeegee speed ($X3$) can be set and directly

(1) *Objective min or max f(x), x = (x1, x2, ..., xd)*
(2) *Initialize a population of n flowers/pollen gametes with random solutions*
(3) *Find the best solution* G_{best}^t *in the initial population*
(4) *Define a switch probability* $p \in [0, 1]$
(5) **while** *(t < MaxGeneration)*
(6) **for** $i = 1{:}n$ (all n flowers in the population)
(7) **If** $rand < p$
(8) Draw a (d-dimensional) set vector L which obeys a Lèvy distribution
(9) Global pollination via $X_i^* = X_i^t + L(G_{\text{best}}^t - X_i^t)$
(10) **else**
(11) Draw ε from a uniform distribution in [0, 1]
(12) Randomly choose j and k among all the solutions
(13) Do local pollination via $X_i^* = X_i^t + \varepsilon(X_j^t - X_k^t)$
(14) **end if**
(15) Evaluate new solutions
(16) If new solutions are better, update them in the population
(17) **end for**
(18) Find the current best solution G_{best}^t
(19) **end while**

Algorithm 1: Flower pollination strategy.

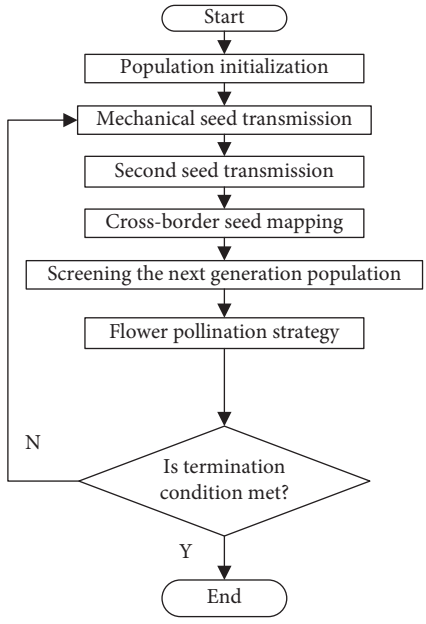

Figure 1: Framework of the EGBO algorithm.

obtained on the 3D additive printing machine. Ink viscosity ($X4$) is obtained by instrument detection before experiment. Ink transfer rate (Y) is obtained by the difference in pulp weight before and after printing.

Table 1 gives the statistical description of the four influencing factors and ultimate binding strength. The scatter plot of each input variable and ink transfer rate is shown in Figure 3. In addition, the entire data set is summarized in Table 2 of this paper.

The experimental work for all problems is done on DELL Inspiron computer with Intel(R) Core (TM) i7-4500U, 2.4 GHz processor and 8 GB of memory running Windows 10. The implementation of experiment is done in MATLAB R2014a tool. EGBO and LSSVM parameters are shown in Table 3.

The model optimization process by EGBO is shown in Figure 4. After 100 iterations, the optimal hyperparameter of the LSSVM prediction model is determined as follows: $\gamma = 3.0373$ and $\sigma = 4.926$.

After further analysis, the data set containing 102 samples is divided into training set (81 samples) and test set (21 samples). After the model is stabilized, the training set samples and test set samples are predicted to obtain the prediction results of ink transfer rate and the real value comparison. Figures 5–8 evaluate the mode's performance on determining ink transfer rate of 3D additive printing based on optimal parameters. The comparison between estimated ink transfer rate and measured ink transfer rate in training and testing phases is shown in Figure 5. As can be seen from the figure, most of the predicted values are close to the actual values. The absolute error and absolute percentage error between estimated and measured ink transfer rate in testing phase are shown in Figure 6. As can be seen from the figure, the absolute error predicted by the model is within 0.01, and the absolute percentage error is within 0.03.

In order to further analyze the performance of the prediction model, another analysis method is used. Figure 7 reports the scatter plot of estimated and measured ink transfer rate in training and testing phases. As shown in Figure 7, we estimated ink transfer rate versus the measured data rise in a straight line with a slope of unity and there is a high number of the estimated data points in the vicinity of the line. In addition, the probability distribution of errors in the model training stage and the test stage is illustrated in Figure 8. As can be seen from the figure, the probability distribution of the error is basically a normal distribution with mean 0.

In order to better verify the capability of the EGBO-LSSVM model, the performance of the hybrid model is

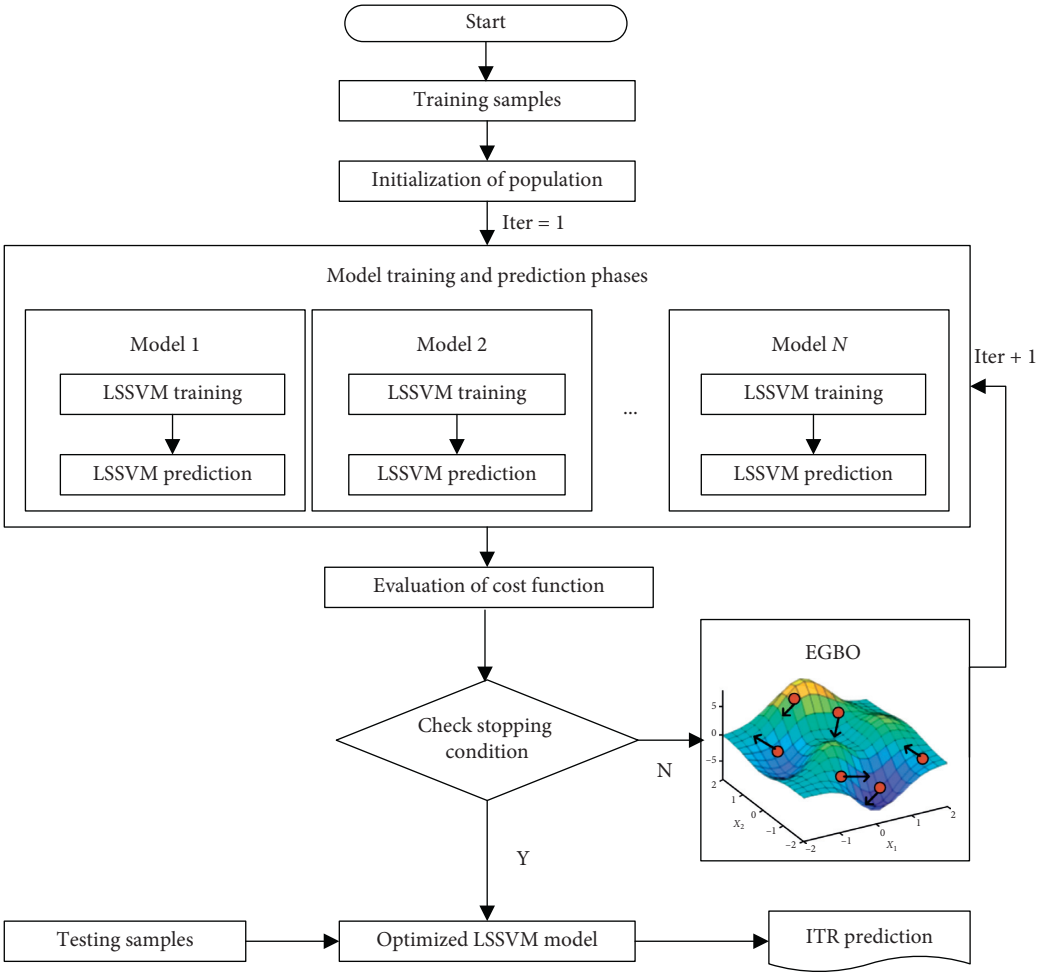

Figure 2: Hybrid EGBO-LSSVM model used for ink transfer rate prediction.

Table 1: Statistical description of variables.

Variables	Notation	Max	Min	Mean	Std	Kurt	Skew
Printing pressure (N)	$X1$	5000	2600	3913.73	586.79	−0.55	−0.67
Squeegee angle (°)	$X2$	20	5	10.49	6.66	−1.46	0.63
Squeegee speed (mm/s)	$X3$	900	400	658.82	159.26	−0.60	−0.47
Ink viscosity (cP)	$X4$	180000	110000	141568.63	25581.29	−1.52	0.25
ITR	Y	0.44	0.21	0.35	0.05	−0.41	−0.41

compared with that of BPANN, MARS, and RegTree [25–27, 28]. BPANN, MARS, and RegTree are effective machine learning methods for modeling nonlinear and multivariate data [29–32].

As mentioned earlier, the data set containing 102 samples is divided into a training set (81) and a test set (21).

In order to offset the randomness of data selection, the EGBO-LSSVM model is executed 20 times and the average results obtained are compared with the other models for the same number of runs. To evaluate the performance of the EGBO-LSSVM model, relative percentage error (MAPE) and determination coefficient (R^2) are used in addition to the RMSE described above [33, 34].

The experimental results of ink transfer rate prediction of the four models are reported in Table 4. From this table, it can be see that EGBO-LSSVM is performing optimally (RMSE = 0.0066, MAPE = 1.6502%, and $R^2 = 0.8476$), followed by MARS (RMSE = 0.0080, MAPE = 2.0296%, and $R^2 = 0.7941$), RegTree (RMSE = 0.0084, MAPE = 2.0915%, and $R^2 = 0.7563$), and BPNN (RMSE = 0.0097, MAPE = 2.3631%, and $R^2 = 0.7467$). It is worth noting that these results are the average of 20 repeated data samples used for model predictions. In addition, the prediction error boxplot of all models is shown in Figure 9.

It is also important to find out statistical significance of EGBO-LSSVM over other comparative models. To quantify

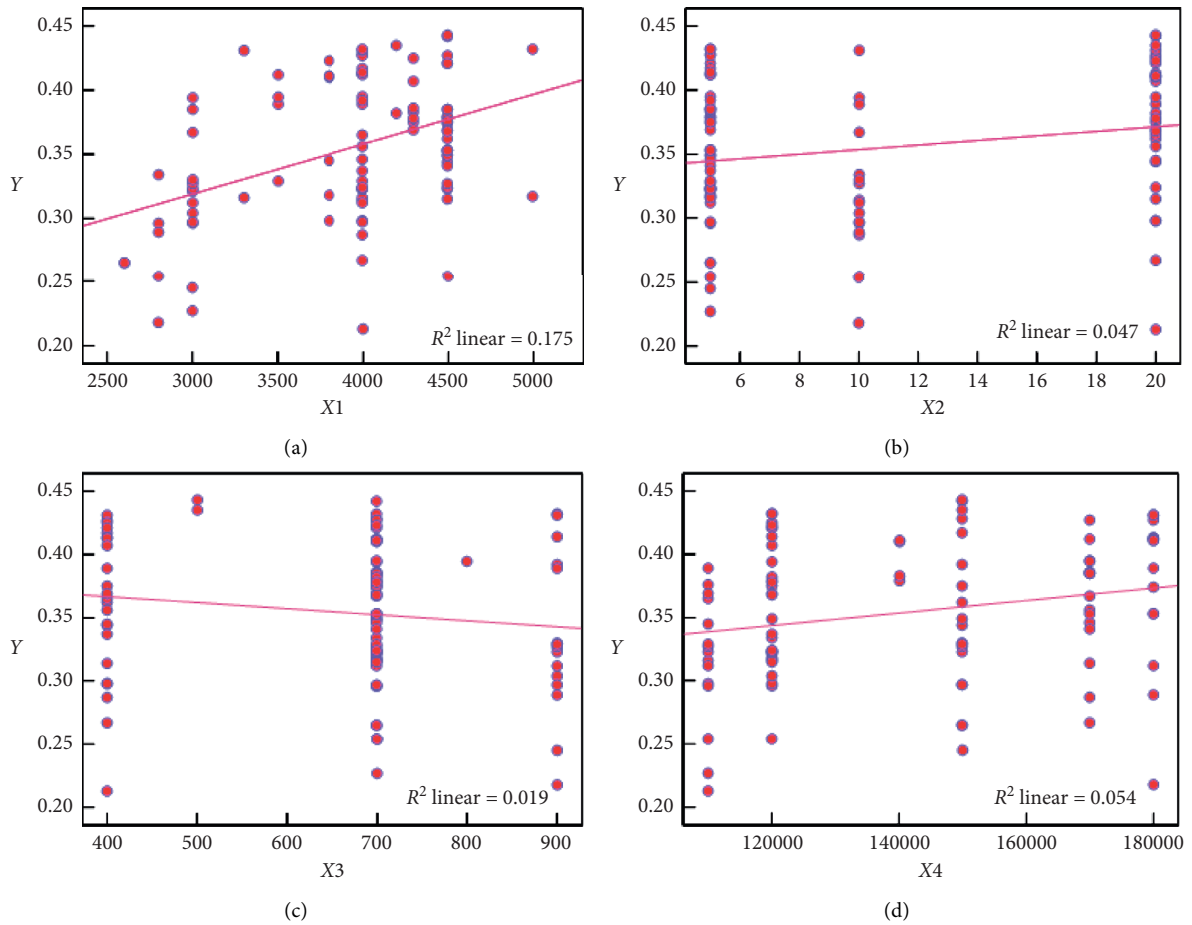

Figure 3: Scatter plots of ink transfer rate w.r.t. different variables.

Table 2: The experimental dataset.

NU	Printing pressure (N)	Squeegee angle (°)	Squeegee speed (mm/s)	Ink viscosity (cP)	Ink transfer rate
1	4000 ()	20	400	170000	0.267
2	4000	10	400	170000	0.314
3	4000	10	400	170000	0.287
4	4000	5	700	110000	0.316
5	4000	5	700	110000	0.312
6	4500	5	700	110000	0.323
7	4500	5	700	120000	0.324
8	4000	5	700	120000	0.323
9	4000	5	700	120000	0.323
10	4000	5	700	120000	0.323
11	5000	5	700	120000	0.317
12	4500	5	700	120000	0.421
13	4500	20	400	150000	0.344
14	4500	20	400	150000	0.362
15	4500	20	400	150000	0.375
16	4000	5	400	150000	0.417
17	4000	5	700	150000	0.428
18	4500	5	700	150000	0.349
19	4500	5	700	120000	0.349
20	5000	5	700	120000	0.432
21	4500	5	700	120000	0.379
22	4500	5	700	140000	0.379
23	4300	5	700	140000	0.383

Table 2: Continued.

NU	Printing pressure (N)	Squeegee angle (°)	Squeegee speed (mm/s)	Ink viscosity (cP)	Ink transfer rate
24	4000	20	400	180000	0.413
25	4000	20	400	180000	0.427
26	4000	20	400	180000	0.431
27	4000	5	700	170000	0.346
28	4300	5	700	170000	0.386
29	4000	20	400	170000	0.356
30	3800	20	400	110000	0.345
31	3800	20	400	110000	0.298
32	4000	20	400	110000	0.213
33	4300	20	400	120000	0.425
34	3000	5	700	120000	0.321
35	3800	5	700	120000	0.318
36	3300	5	700	120000	0.316
37	3000	10	700	120000	0.394
38	2800	5	700	120000	0.296
39	2600	5	700	150000	0.265
40	2600	5	700	150000	0.265
41	3000	5	900	150000	0.323
42	4500	20	700	150000	0.442
43	4500	20	500	150000	0.443
44	4200	20	500	150000	0.435
45	4000	20	400	120000	0.298
46	2800	10	700	120000	0.334
47	3000	10	700	170000	0.367
48	3000	5	700	170000	0.385
49	3500	5	700	170000	0.412
50	2800	10	700	110000	0.254
51	3000	10	700	110000	0.296
52	3000	5	700	110000	0.227
53	4000	5	400	180000	0.413
54	4000	5	700	180000	0.412
55	4500	5	700	180000	0.374
56	4500	5	700	180000	0.353
57	4500	5	700	180000	0.353
58	4500	5	700	170000	0.427
59	4500	5	700	170000	0.353
60	4500	5	700	170000	0.341
61	4500	5	700	110000	0.327
62	4000	20	400	110000	0.389
63	4000	20	400	110000	0.365
64	4000	5	400	120000	0.337
65	4000	5	700	120000	0.323
66	4000	5	700	170000	0.395
67	4500	5	700	170000	0.385
68	4500	5	700	170000	0.385
69	4500	5	700	110000	0.376
70	4500	5	700	110000	0.369
71	4000	5	700	110000	0.329
72	4300	5	700	120000	0.375
73	4300	20	400	120000	0.369
74	4300	20	400	120000	0.407
75	4500	20	400	120000	0.421
76	4500	5	700	120000	0.254
77	4000	5	700	150000	0.297
78	4000	20	700	120000	0.324
79	4500	20	700	120000	0.315
80	4200	20	700	120000	0.382
81	4300	20	700	120000	0.378
82	4500	20	700	120000	0.368
83	3000	10	900	120000	0.304

Table 2: Continued.

NU	Printing pressure (N)	Squeegee angle (°)	Squeegee speed (mm/s)	Ink viscosity (cP)	Ink transfer rate
84	3000	10	900	150000	0.297
85	3000	5	900	150000	0.245
86	4000	5	900	150000	0.392
87	3000	10	900	150000	0.327
88	3000	10	900	150000	0.33
89	3500	5	900	150000	0.329
90	4000	5	900	120000	0.414
91	4000	5	900	120000	0.432
92	3800	20	700	120000	0.423
93	3800	20	700	140000	0.41
94	3800	20	700	140000	0.411
95	3800	20	700	180000	0.411
96	3800	20	700	180000	0.411
97	3000	10	900	180000	0.312
98	2800	10	900	180000	0.289
99	3500	10	900	180000	0.389
100	3300	10	900	180000	0.431
101	2800	10	900	180000	0.218
102	3500	20	800	170000	0.3945

Table 3: The parameter values of the EGBO algorithm.

Symbol	Quantity	Value
N_{init}	Number of initial population	5
$\text{iter}_{\max}$	Maximum number of iterations	100
d	Problem dimension	2
$N_{\max}$	Maximum number of plant population	50
$s_{\max}$	Maximum number of seeds	5
$s_{\min}$	Minimum number of seeds	1
n	Nonlinear modulation index	3
N_{sec}	Number of second transmission	5
F	Zoom factor	2
A_{init}	Initial value of diffusion amplitude	10
p	Switch probability	0.8

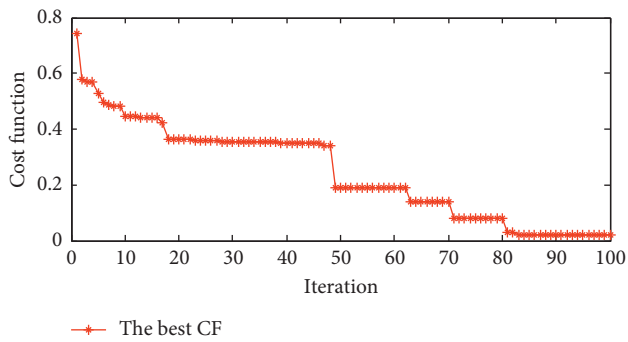

Figure 4: Convergence of the EGBO-LSSVM model.

the performance of the models statistically, the Wilcoxon symbolic rank test is used to better confirm the statistical significance of the superiority of EGBO-LSSVM. The p value calculated by the test is shown in Table 5 (preselection threshold = 0.05). The results depict the pairwise p value obtained from the Wilcoxon symbolic rank test for all models. It is observed from the results that EGBO-LSSVM and MARS are statistically similar for obtaining RMSE and MAPE values. In addition to that, a significant statistical difference has been observed in the results of the EGBO-LSSVM and other competitive models for obtaining the RMSE, MAPE, and the R^2 values.

In addition, to assess the sensitivity of input variables to the performance of the EGBO-LSSVM model, the Fourier amplitude sensitivity test (FAST) [35, 36] is used in this study. This study relies on a toolkit developed by Pianosi et al. [37, 38] to implement the FAST method. Based on the fast method, the variation of ink transfer rate prediction is decomposed into partial variances of input factors by Fourier transform. The influence of input characteristics on the output of EGBO-LSSVM can be quantified by the first-order sensitivity index (FOSI) [39]. The sensitivity analysis results are shown in Figure 10.

As can be seen from Figure 10, $X1$ (FOSI = 49.32%) has the greatest impact on the model prediction results, followed by $X4$ (FOSI = 20.32%), $X2$ (FOSI = 18.45%), and $X3$ (FOSI = 11.49%). From the analysis results, it can be seen that all the characteristics have certain influence on the prediction of EGBO-LSSVM.

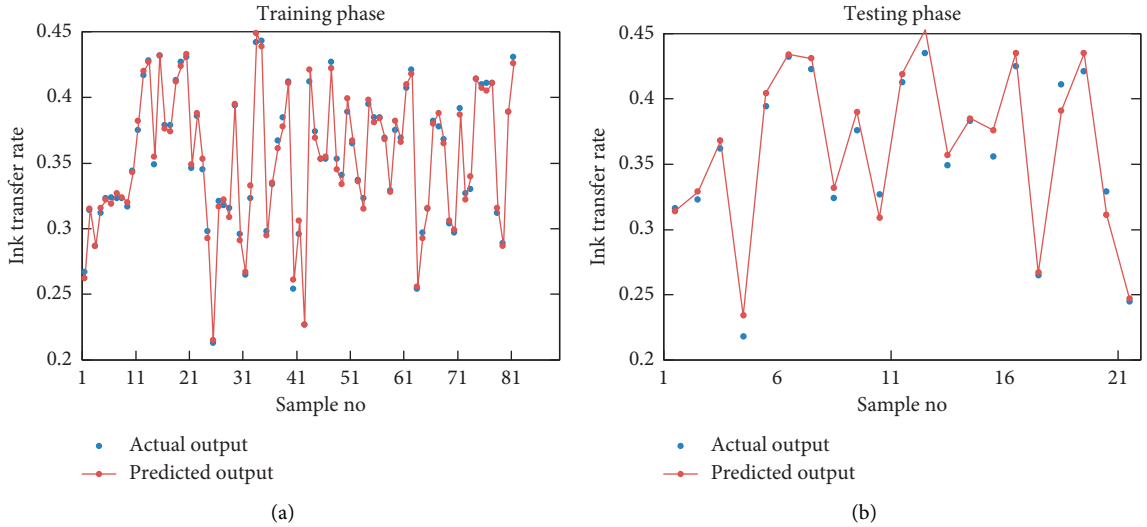

Figure 5: Comparison between estimated and measured ink transfer rate in training and testing phases.

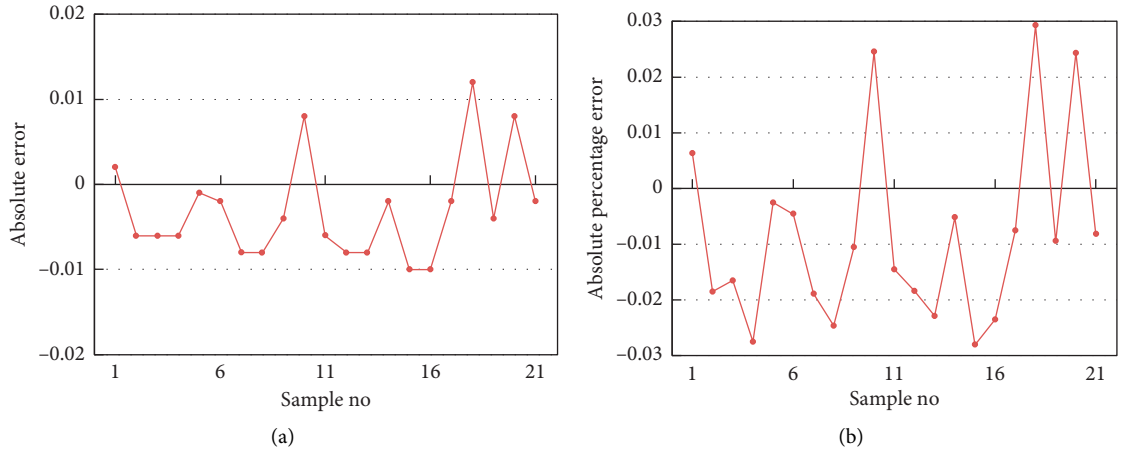

Figure 6: Error between estimated and measured ink transfer rate in the testing phase: (a) absolute error and (b) absolute percentage error.

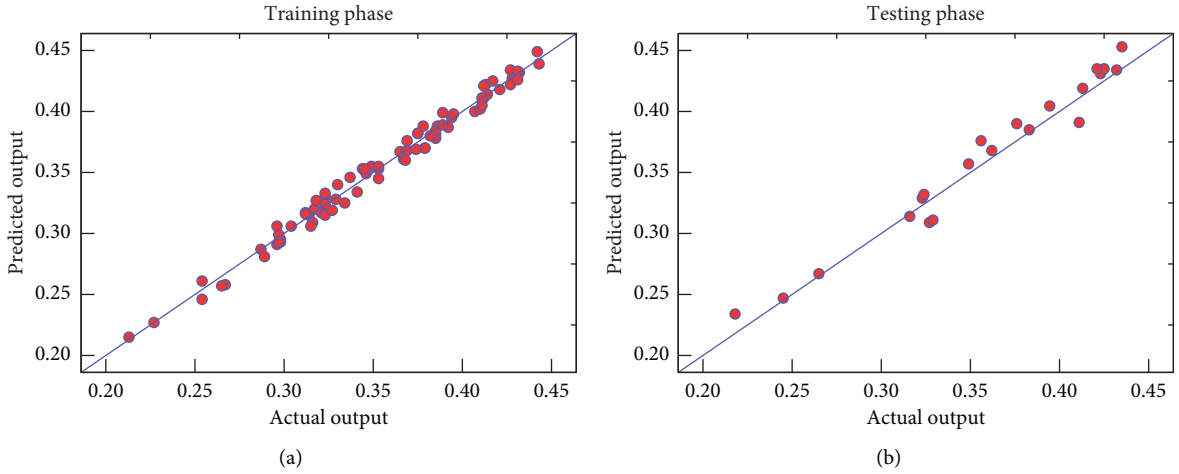

Figure 7: Scatter plot of estimated and measured ink transfer rate in training and testing phases.

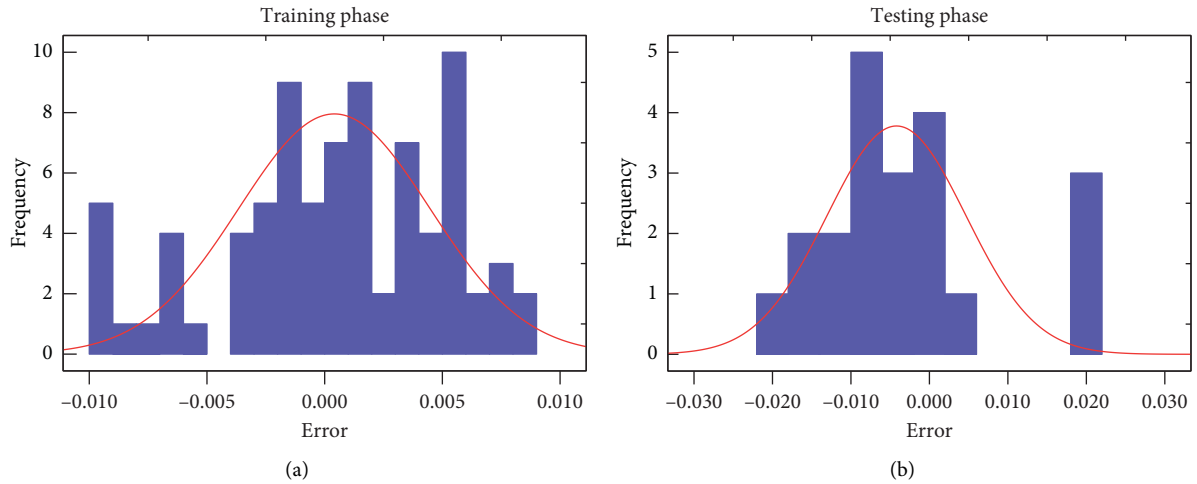

Figure 8: Histograms of the model prediction error in training and testing phases.

Table 4: Comparative results of various methods averaged over 20 runs.

Phase	Metrics	EGBO-LSSVM		BPANN		MARS		RegTree	
		Mean	Std	Mean	Std	Mean	Std	Mean	Std
Training	RMSE	0.0047	0.04	0.0110	0.53	0.0073	0.12	0.0088	0.19
	MAPE (%)	1.0247	0.45	3.7913	7.82	2.1734	2.11	3.1429	2.82
	R^2	0.9470	0.03	0.7908	0.06	0.8982	0.03	0.8591	0.03
Testing	RMSE	0.0066	0.42	0.0097	0.67	0.0080	0.61	0.0084	0.75
	MAPE (%)	1.6502	2.83	2.3631	5.28	2.0296	4.17	2.0915	5.41
	R^2	0.8476	0.14	0.7467	0.16	0.7941	0.14	0.7563	0.21

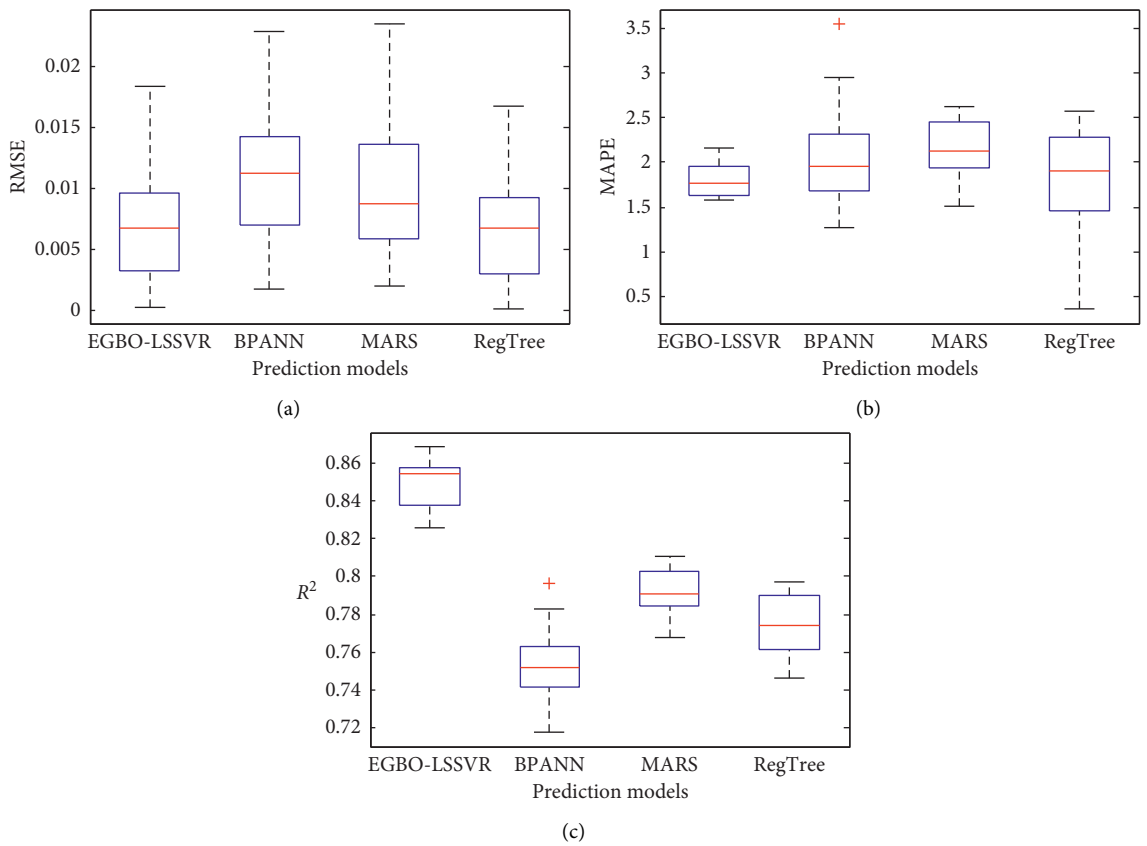

Figure 9: Box plots of prediction models.

Table 5: Wilcoxon signed-rank test for the "RMSE," "MAPE," and the "R^2" values obtained.

Test for RMSE		Test for MAPE		Test for R^2	
Algorithm	p value	Algorithm	p value	Algorithm	p value
1-2	$3.07E-06$	1-2	0.0050142	1-2	0.001481
1–3	0.07204543	1–3	0.0478682	1–3	0.000129
1–4	$3.29E-05$	1–4	0.0016747	1–4	0.009786

*1, EGBO-LSSVM; 2, BPANN; 3, MARS; 4, RegTree.

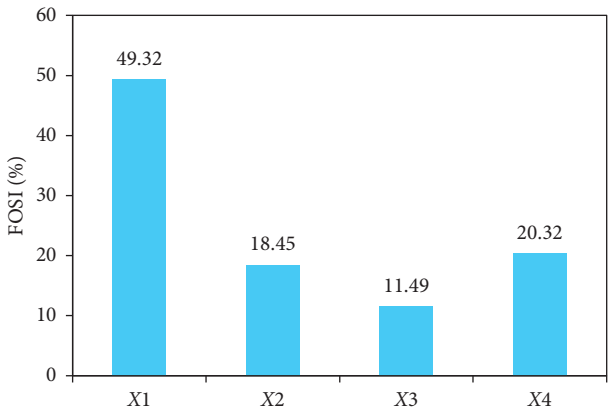

Figure 10: First-order sensitivity index (FOSI) of variables.

5. Conclusion

In this study, a model is developed and proposed in order to predict ink transfer rate in 3D additive printing by printing pressure, squeegee angle, squeegee speed, and ink viscosity as influential parameters. The conclusion can be summarized as follows:

(1) The high viability and capability of LSSVM approach with RBF kernel to calculate ink transfer rate in 3D additive printing are proven based on the available experimental data.

(2) Hyperparameters, including γ and σ, have a significant effect on LSSVM training results and generalization ability. By applying the EGBO algorithm, the optimal values of γ and σ are found to be equal to 3.0373 and 4.926, respectively.

(3) A hybrid model of LSSSVM and EGBO provides an appropriate tool to predict ink transfer rate in 3D additive printing. The outputs of the model had good agreement with the experimental data. The determination coefficients, the root-mean-squared errors, and the mean absolute percentage errors of the model are 0.8476, 6.6×10 (−3), and 1.6502×10 (−3), respectively.

Data Availability

The data used to support the findings of this study are included within the article.

Conflicts of Interest

The authors declare that there are no conflicts of interest regarding the publication of this paper.

Acknowledgments

This work was partially supported by the Natural Science Foundation of China (5147509) and the National Key R&D Program of China (2018YFB1308800).

References

[1] R. Durairaj, T. A. Nguty, and N. N. Ekere, "Critical factors affecting paste flow during the stencil printing of solder paste," *Soldering & Surface Mount Technology*, vol. 13, no. 2, pp. 30–34, 2001.

[2] D. J. Clements, M. P. Y. Desmulliez, and E. Abraham, "The evolution of paste pressure during stencil printing," *Soldering & Surface Mount Technology*, vol. 19, no. 9, pp. 9–14, 2007.

[3] J. Kim and E. Jeon, "Process parameter optimization of screen printing device for vacuum glazing pillar array," *Journal of Advanced Mechanical Design, Systems, and Manufacturing*, vol. 9, no. 5, 2015.

[4] Y. Wang, P. Li, Z. Sun, and Y. Sun, "A model of screen reaction force for the 3D additive screen printing," *The Journal of the Textile Institute*, vol. 109, no. 8, pp. 1000–1007, 2018.

[5] Y. Wang, Y. Liu, and Y. Sun, "A hybrid intelligence technique based on the Taguchi method for multi-objective process parameter optimization of the 3D additive screen printing of athletic shoes," *Textile Research Journal*, vol. 90, no. 9-10, pp. 1067–1083, 2020.

[6] H. A. Afan, A. El-Shafie, Z. M. Yaseen, M. M. Hameed, W. H. M. Wan Mohtar, and A. Hussain, "ANN based sediment prediction model utilizing different input scenarios," *Water Resources Management*, vol. 29, no. 4, pp. 1231–1245, 2015.

[7] F. M. S. Al-Zwainy, R. I. K. Zaki, A. M. Al-saadi, and H. F. Ibraheem, "Validity of artificial neural modeling to estimate time-dependent deflection of reinforced concrete beams," *Cogent Engineering*, vol. 5, pp. 1–15, 2018.

[8] D.-K. Bui, T. Nguyen, J.-S. Chou, H. Nguyen-Xuan, and T. D. Ngo, "A modified firefly algorithm-artificial neural network expert system for predicting compressive and tensile strength of high-performance concrete," *Construction and Building Materials*, vol. 180, pp. 320–333, 2018.

[9] W. Chen, X. Xie, J. Wang et al., "A comparative study of logistic model tree, random forest, and classification and

regression tree models for spatial prediction of landslide susceptibility," *Catena*, vol. 151, pp. 147–160, 2017.

[10] M.-Y. Cheng and N.-D. Hoang, "Estimating construction duration of diaphragm wall using firefly-tuned least squares support vector machine," *Neural Computing and Applications*, vol. 30, no. 8, pp. 2489–2497, 2018.

[11] S. Faizollahzadeh Ardabili, B. Najafi, S. Shamshirband, B. Minaei Bidgoli, R. C. Deo, and K.-w. Chau, "Computational intelligence approach for modeling hydrogen production: a review," *Engineering Applications of Computational Fluid Mechanics*, vol. 12, no. 1, pp. 438–458, 2018.

[12] W. Książek, M. Abdar, U. R. Acharya, and P. Pławiak, "A novel machine learning approach for early detection of hepatocellular carcinoma patients," *Cognitive Systems Research*, vol. 54, pp. 116–127, 2019.

[13] Y. Wang, Y. Liu, Z. Meng, and Y. Sun, "Optimization of process parameters for 3D additive screen printing based on genetic algorithm and neural network," *Journal of Textile Research*, vol. 40, no. 11, pp. 168–174, 2019.

[14] P. Pławiak, "Novel methodology of cardiac health recognition based on ECG signals and evolutionary-neural system," *Expert Systems with Applications*, vol. 92, pp. 334–349, 2018.

[15] S. Deng, X. Wang, Y. Zhu, F. Lv, and J. Wang, "Hybrid grey wolf optimization algorithm based support vector machine for groutability prediction of fractured rock mass," *Journal of Computing in Civil Engineering*, vol. 33, Article ID 04018065, 2019.

[16] M. H. Ahmadi, M. A. Ahmadi, M. A. Nazari, O. Mahian, and R. Ghasempour, "A proposed model to predict thermal conductivity ratio of Al_2O_3/EG nanofluid by applying least squares support vector machine (LSSVM) and genetic algorithm as a connectionist approach," *Journal of Thermal Analysis and Calorimetry*, vol. 135, no. 1, pp. 271–281, 2019.

[17] B. Yan, H. Cui, H. Fu, J. Zhou, and H. Wang, "A new method for feature extraction and classification of single-stranded DNA based on collaborative filter," *Mathematical Problems in Engineering*, vol. 2020, Article ID 3876367, 10 pages, 2020.

[18] S. Li and Y. Sun, "Garden balsam optimization algorithm," *Concurrency & Computation Practice & Experience*, vol. 32, no. 2, 2020.

[19] J. Suykens, J. V. Gestel, J. D. Brabanter, B. D. Moor, and J. Vandewalle, *Least Squares Support Vector Machines*, World Scientific, Hackensack, NJ, USA, 2002.

[20] H. N. Rad, M. Hasanipanah, M. Rezaei, and A. L. Eghlim, "Developing a least squares support vector machine for estimating the blast-induced flyrock," *Engineering with Computers*, vol. 34, no. 4, pp. 709–717, 2017.

[21] F. Deng, Y. He, S. Zhou, Y. Yu, H. Cheng, and X. Wu, "Compressive strength prediction of recycled concrete based on deep learning," *Construction and Building Materials*, vol. 175, pp. 562–569, 2018.

[22] S. Li, H. Fang, and X. Liu, "Parameter optimization of support vector regression based on sine cosine algorithm," *Expert Systems with Applications*, vol. 91, pp. 63–77, 2018.

[23] M. A. Al-Betar, M. A. Awadallah, I. A. Doush, A. I. Hammouri, M. Mafarja, and Z. A. A. Alyasseri, "Island flower pollination algorithm for global optimization," *The Journal of Supercomputing*, vol. 75, pp. 1–44, 2019.

[24] M. A. Awadallah, M. A. Al-Betar, A. L. A. Bolaji, E. M. Alsukhni, and H. Al-Zoubi, "Natural selection methods for artificial bee colony with new versions of onlooker bee," *Soft Computing*, vol. 23, no. 15, pp. 6455–6494, 2019.

[25] S. Heddam and O. Kisi, "Modelling daily dissolved oxygen concentration using least square support vector machine, multivariate adaptive regression splines and M5 model tree," *Journal of Hydrology*, vol. 559, pp. 499–509, 2018.

[26] V. Amaratunga, L. Wickramasinghe, A. Perera, J. Jayasinghe, and U. Rathnayake, "Artificial neural network to estimate the paddy yield prediction using climatic data," *Mathematical Problems in Engineering*, vol. 2020, Article ID 8627824, 11 pages, 2020.

[27] Y. Lu, H. Jiang, T. Liao, C. Xu, and C. Deng, "Characteristic analysis and modeling of network traffic for the electromagnetic launch system," *Mathematical Problems in Engineering*, vol. 2019, Article ID 2929457, 7 pages, 2019.

[28] P. Taherei Ghazvinei, H. Hassanpour Darvishi, A. Mosavi et al., "Sugarcane growth prediction based on meteorological parameters using extreme learning machine and artificial neural network," *Engineering Applications of Computational Fluid Mechanics*, vol. 12, no. 1, pp. 738–749, 2018.

[29] A. Gholampour, I. Mansouri, O. Kisi, and T. Ozbakkaloglu, "Evaluation of mechanical properties of concretes containing coarse recycled concrete aggregates using multivariate adaptive regression splines (MARS), M5 model tree (M5Tree), and least squares support vector regression (LSSVR) models," *Neural Computing & Applications*, vol. 32, pp. 295–308, 2018.

[30] A. T. C. Goh, W. Zhang, Y. Zhang, Y. Xiao, and Y. Xiang, "Determination of earth pressure balance tunnel-related maximum surface settlement: a multivariate adaptive regression splines approach," *Bulletin of Engineering Geology and the Environment*, vol. 77, no. 2, pp. 489–500, 2018.

[31] K.-W. Liao, N.-D. Hoang, and J. Gitomarsono, "A probabilistic safety evaluation framework for multi-hazard assessment in a bridge using SO-MARS learning model," *KSCE Journal of Civil Engineering*, vol. 22, no. 3, pp. 903–915, 2018.

[32] C. Qi, A. Fourie, and X. Zhao, "Back-analysis method for stope displacements using gradient-boosted regression tree and firefly algorithm," *Journal of Computing in Civil Engineering*, vol. 32, Article ID 04018031, 2018.

[33] V. H. Nhu, N. D. Hoang, V. B. Duong, H. D. Vu, and D. Tien Bui, "A hybrid computational intelligence approach for predicting soil shear strength for urban housing construction: a case study at Vinhomes Imperia project, Hai Phong City," *Engineering with Computers*, vol. 36, no. 2, pp. 603–616, 2019.

[34] D. Tien Bui, V.-H. Nhu, and N.-D. Hoang, "Prediction of soil compression coefficient for urban housing project using novel integration machine learning approach of swarm intelligence and multi-layer perceptron neural network," *Advanced Engineering Informatics*, vol. 38, pp. 593–604, 2018.

[35] H. Luo and S. G. Paal, "Machine learning-based backbone curve model of reinforced concrete columns subjected to cyclic loading reversals," *Journal of Computing in Civil Engineering*, vol. 32, Article ID 04018042, 2018.

[36] R. Moazenzadeh, B. Mohammadi, S. Shamshirband, and K.-w. Chau, "Coupling a firefly algorithm with support vector regression to predict evaporation in northern Iran," *Engineering Applications of Computational Fluid Mechanics*, vol. 12, no. 1, pp. 584–597, 2018.

[37] F. Pianosi, F. Sarrazin, and T. Wagener, "A matlab toolbox for global sensitivity analysis," *Environmental Modelling & Software*, vol. 70, pp. 80–85, 2015.

[38] F. Pianosi, F. Sarrazin, and T. Wagener, "SAFE Toolbox," 2019, https://www.safetoolboxinfo/about-us/.

[39] N.-D. Hoang, "Estimating punching shear capacity of steel fibre reinforced concrete slabs using sequential piecewise multiple linear regression and artificial neural network," *Measurement*, vol. 137, pp. 58–70, 2019.